Single-Shot Diffusion Tensor Spectroscopic Imaging in Human Brain

Stefan Posse[1,2], Kevin F Tagne[3], and Stephen R Dager[4]

[1]Neurology, U New Mexico, Albquerque, NM, United States, [2]Physics and Astronomy, U New Mexico, Albuquerque, NM, United States, [3]Neurology, U New Mexico, Albuquerque, NM, United States, [4]Radiology, U Washington, Seattle, WA, United States

TARGET AUDIENCE: MR scientists and clinical researchers in the fields of neurology and spectroscopy.

PURPOSE: Metabolite diffusion can provide unique information on intracellular properties, such as viscosity, cell swelling, restriction in subcellular structures, and cytoplasmic streaming that is complementary to water diffusion that averages across the intra- and extracellular compartments. Metabolite diffusion may help to characterize intracellular microstructural changes of the healthy human brain as it ages, abnormalities in cellular organization and axonal structure in patients with autism, possible inflammatory processes in ischemia and multiple sclerosis, and brain tumors[1,2]. Most human studies thus far investigating metabolite diffusion have used single voxel methods[3-7] due to overwhelming motion sensitivity of conventional MR spectroscopic imaging (MRSI) techniques[8]. Using navigator-based correction of motion artifacts we[9,10] and Ercan et al.[11] have recently demonstrated feasibility of mapping metabolite diffusion in a central PRESS-localized brain region. However, there is an urgent need to develop single-shot diffusion tensor spectroscopic imaging (DTSI) methods to fully address the motion sensitivity of conventional DTSI and map metabolite diffusion across extended brain areas to correlate with DTI. In this study we develop a single-shot narrow-bandwidth proton-echo-planar-spectroscopic-imaging (PEPSI) method with cardiac-gating and navigator correction to measure the diffusion tensor of water, Cho, Cr and NAA across an entire slice.

METHOD: The slice-selective PEPSI-based DTSI pulse sequence employs three WET water suppression modules and suppression of regions with subcutaneous fat using 8 outer volume suppression slice. Spatial-spectral encoding was performed using a series of double-sampled EPI readout modules for separate processing of even and odd echo data as described in. A frequency selective refocusing RF pulse was used to suppress spectral signal outside of the spectral width of the spatial-spectral encoding module. Diffusion gradients with 25 ms duration, 47 ms separation and 23 mT/m maximum amplitude were applied along two spatial axes. Peripheral gating with a time delay of 250 msec between the systolic wave and the beginning of the pulse sequence was used to compensate for cardiac-related brain and cerebrospinal fluid pulsations. Correction of movement-related phase instability in individual acquisitions was performed on a coil-by-coil basis following the approach described in[12], using up to 4 navigator acquisitions during the water suppression modules, after excitation and immediately before the phase encoding gradients and the echo-planar readout train. The navigator acquisition was spatially localized using a pair of echo-planar gradients oriented perpendicular to the PEPSI slice and employed automatic detection of the center of the PEPSI slice across the multi-coil data by enforcing consistency between multi-coil data. Relaxation correction was applied on a TR-by-TR basis to account for differences in scan time between individual data sets as a result of heart rate related variability in TR. Navigator correction, spatial-spectral reconstruction with multi-coil combination and phase correction was performed online on the scanner as described in[8]. Four healthy subjects (2 female, 2 male, aged 20 to 56 years) participated after giving institutionally reviewed informed consent. Data were collected on a clinical 3T TIM Trio scanner (Siemens Medical Solutions, Inc) equipped with a 32-channel head array coil. 2D DTSI data were collected from a supraventricular 20 mm thick slice in AC/PC orientation using: TE: 90 ms, TR: 4 s, refocusing RF pulse bandwidth: 1.54 ppm centered at 2.0, 3.1 or 4.65 ppm, encoded spectral width: 0.77 ppm, b-values: 0 and 1820 s/mm^2, 6 gradient directions, FOV: 226x226 mm^2, spatial matrix: 16x16 voxels, nominal voxel size: 4 cm^3, using single average in case of water and 32 averages in case of metabolites, resulting in nominal scan times of 4 s and 2:24 min, respectively. One non diffusion-weighted data set was acquired using a refocusing RF pulse bandwidth of 2 ppm centered at 2.6 ppm. The total scan time to collect 7 water-suppressed and 7 non-water-suppressed data sets was approximately 20 minutes. Spectral quantification of Cho, Cr, NAA and tissue water was performed using LCModel fitting[13] with an analytically modeled basis set. The diffusion tensor, the Trace/3 ADC (mean diffusivity), the fractional anisotropy (FA) and relative anisotropy (RA) were computed using MedINRIA software.

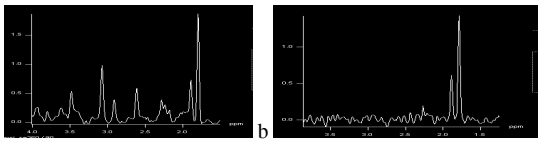

Fig. 1: Conventional PEPSI spectrum in a phantom (a) without and (b) with frequency selective refocusing at 2.0 ppm.

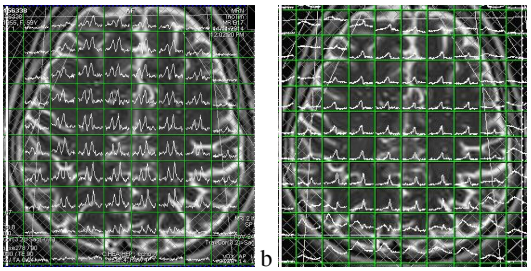

Fig. 2: Single-shot PEPSI data reconstructed on the scanner showing (a) Cho and Cr and (b) NAA at b=1820 s/mm^2.

RESULTS: Frequency selective refocusing at 2.0 and 3.1 ppm using a conventional PEPSI sequence suppressed signals outside of the refocusing bandwidth to the noise level (**Fig. 1**). Mean Trace/3 ADC values of Cho (0.89+/-0.06*10^{-3} mm^2/s), Cr (0.82+/-0.16*10^{-3} mm^2/s) and NAA (0.9+/-0.26*10^{-3} mm^2/s) in a phantom at 20^0 C were consistent with our previous study[1]. Spatial and spectral ghosting in vivo was negligible (**Fig. 2**). Some scans with diffusion gradients along the Z-axis displayed relative decreases in signal intensity in frontal brain regions, which may reflect inter-average phase shifts and intra-voxel signal dephasing due to rotational movement. Water Trace/3 ADC maps show distinction between gray and white matter (**Fig. 3b**). Metabolite Trace/3 ADC maps were less spatially distinct in gray and white matter, in part due to limitations in SNR (**Fig. 3c-e**). Slice averaged Trace/3 ADC and FA values of Cho, Cr, NAA and tissue water were in the ranges reported in previous studies using single voxel methods[4-6] and using diffusion tensor MRI (**Table 1**). Data collection in a larger number of subjects using multiple slice locations is in progress to assess the feasibility of multi-slice DTSI in the entire brain.

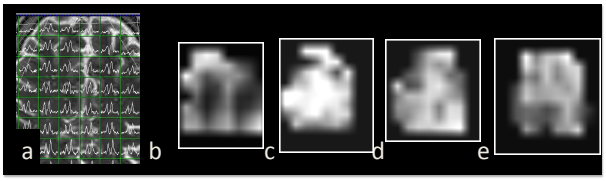

Figure 3: Single-shot PEPSI data reconstructed on the scanner showing (a) Cho and Cr and (b) NAA at b=1820 s/mm^2 and (c)

	H2O		Cho		Cr		NAA	
	mean	SD	mean	SD	mean	SD	mean	SD
Trace/3 ADC *10-3 [mm2/s]	0.74	0.16	0.20	0.08	0.19	0.05	0.19	0.08
FA	0.21	0.12						

Table 1: Slice averaged results in a single subject.

DISCUSSION: This study demonstrates feasibility of single-shot 2D-DTSI in human brain, which completely suppresses localization artifacts. However, in contrast to DTI this DTSI method retains sensitivity to rotational movement due to the large voxels size, which will be addressed in future studies by tracking displacement in k-space using spatially resolved navigators along all spatial directions, by increasing the sensitivity of the navigator correction using stronger residual water signals and by optimizing phase coherent averaging. We are also investigating single-shot encoding at higher spatial resolution, multi-slice acquisition and parallel imaging[14] and the combination of compressed sensing and parallel imaging, which as we have recently demonstrated accelerates PEPSI and increases the spatial resolution and the narrow spectral width in single-shot DTSI[15].

CONCLUSION: Single-shot DTSI substantially reduces motion sensitivity compared with phase encoded DTSI techniques, but sensitivity to rotational movement remains due to the large voxel size. Improved navigator approaches to address this limitation are under development. Single-shot DTSI in conjunction with DTI may provide an improved understanding of disease-related changes in tissue microstructure properties.

REFERENCES: [1] E. T. Wood, et al. *J Neurosci.,* 32, 6665, 2012. [2] M. Harada, et al. *NMR Biomed,* 15, 69, 2002. [3] S. Posse, et al., *Radiology,* 188, 719, 1993. [4] J. Ellegood, et al., *Magn Reson Med,* 55, 1, 2006. [5] J. Upadhyay, et al., *Magn Reson Med,* 58, 1045, 2007. [6] J. Ellegood, et al., *Magn Reson Med,* 53, 1025, 2005. [7] H. E. Kan, et al., *Magn Reson Med,* 67, 1203, 2012. [8] S. Posse, et al., *Magn Reson Med,* 58, 236, 2007. [9] S. Posse et al., Proc. ISMRM 2013, 3956. [10] A. Landow et al., Proc. ISMRM 2014, 696. [11] A.E. Ercan et al., *Magn Reson Med,* 2014 (in press). [12] S. Posse, et al., *J Magn. Reson. Series B,* 102, 222, 1993. [13] S. W. Provencher, *Magn. Reson. Med.,* 30, 672, 1993. [14] S. Posse, et al. *Magn Reson Med,* 61, 541, 2009. [15] R. Otazo et al. Proc. ISMRM 2009.

ACKNOWLEDGEMENTS: Funded by NIH grant 1R21EB011606.